THE JOURNAL OF PHYSICAL CHEMISTRY A

Article

pubs.acs.org/JPCA

Singlet−Triplet Energy Gaps for Diradicals from Particle−Particle Random Phase Approximation

Yang Yang,[†] Degao Peng,[†] Ernest R. Davidson,[‡] and Weitao Yang*[,†,¶,§]

[†]Department of Chemistry, and [¶]Department of Physics, Duke University, Durham, North Carolina 27708, United States

[‡]Department of Chemistry, University of Washington, Seattle, Washington 98195, United States

[§]Key Laboratory of Theoretical Chemistry of Environment, Ministry of Education, School of Chemistry and Environment, South China Normal University, Guangzhou 510006, China

Supporting Information

ABSTRACT: The particle−particle random phase approximation (pp-RPA) for calculating excitation energies has been applied to diradical systems. With pp-RPA, the two nonbonding electrons are treated in a subspace configuration interaction fashion while the remaining part is described by density functional theory (DFT). The vertical or adiabatic singlet−triplet energy gaps for a variety of categories of diradicals, including diatomic diradicals, carbene-like diradicals, disjoint diradicals, four-π-electron diradicals, and benzynes are calculated. Except for some excitations in four-π-electron diradicals, where four-electron correlation may play an important role, the singlet−triplet gaps are generally well predicted by pp-RPA. With a relatively low $O(r^4)$ scaling, the pp-RPA with DFT references outperforms spin-flip configuration interaction singles. It is similar to or better than the (variational) fractional-spin method. For small diradicals such as diatomic and carbene-like ones, the error of pp-RPA is slightly larger than noncollinear spin-flip time-dependent density functional theory (NC-SF-TDDFT) with LDA or PBE functional. However, for disjoint diradicals and benzynes, the pp-RPA performs much better and is comparable to NC-SF-TDDFT with long-range corrected ωPBEh functional and spin-flip configuration interaction singles with perturbative doubles (SF-CIS(D)). In particular, with a correct asymptotic behavior and being almost free from static correlation error, the pp-RPA with DFT references can well describe the challenging ground state and charge transfer excitations of disjoint diradicals in which almost all other DFT-based methods fail. Therefore, the pp-RPA could be a promising theoretical method for general diradical problems.

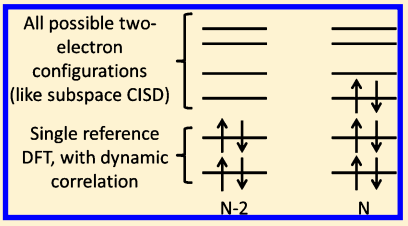

INTRODUCTION

Diradicals are molecules with two electrons in degenerate or nearly degenerate molecular orbitals.[1,2] They can be short-lived reactive species that play an important role in chemical reactions, such as carbenes.[3] They can also be relatively stable species that can possibly be used in material sciences, such as graphene fragments.[4] In a diradical, the various possibilities of alignments for the two nonbonding electrons give rise to its versatile chemistry behaviors. Therefore, it is of particular interest to study diradicals both experimentally and theoretically.

In the simplest two-orbital diradical model, there are six possible occupation configurations corresponding to six determinants (Figure 1). Through linear combination, six spin-adapted configurations can be generated. Of these six spin-adapted ones, there are three triplet states with the same energy and three singlet states usually with different energies.

In a simple Hartree−Fock (HF) analysis, the alignment of these four energy levels depends on the orbital energies, the coulomb repulsion energy within the same orbital and between the two orbitals, as well as the exchange energy between the two orbitals.

In general, if we ignore the symmetry and consider all the possible configuration interactions within the two-orbital two-electron model, there is a general form for the three singlet states,

$$\begin{aligned}|\Psi\rangle &= c_{aa}|a\bar{a}\rangle + c_{bb}|b\bar{b}\rangle + \frac{c_{ab}}{\sqrt{2}}(|a\bar{b}\rangle - |\bar{a}b\rangle)\\ &= \frac{c_{aa}+c_{bb}}{2}(|a\bar{a}\rangle + |b\bar{b}\rangle) + \frac{c_{aa}-c_{bb}}{2}(|a\bar{a}\rangle - |b\bar{b}\rangle)\\ &\quad + \frac{c_{ab}}{\sqrt{2}}(|a\bar{b}\rangle - |\bar{a}b\rangle)\\ &= C_1\Phi_1 + C_2\Phi_2 + C_3\Phi_3, \end{aligned} \tag{1}$$

with

$$\Phi_1 = \frac{|a\bar{a}\rangle + |b\bar{b}\rangle}{\sqrt{2}} \tag{2a}$$

$$\Phi_2 = \frac{|a\bar{a}\rangle - |b\bar{b}\rangle}{\sqrt{2}} \tag{2b}$$

$$\Phi_3 = \frac{|a\bar{b}\rangle - |\bar{a}b\rangle}{\sqrt{2}} \tag{2c}$$

Received: December 20, 2014
Revised: April 15, 2015
Published: April 20, 2015

DOI: 10.1021/jp512727a
J. Phys. Chem. A 2015, 119, 4923−4932

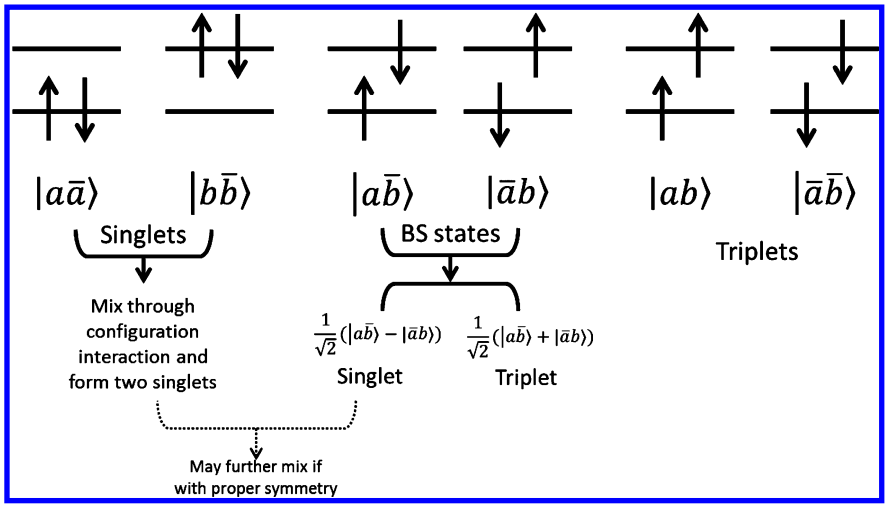

Figure 1. Two-orbital diradical model. Of the six possible configurations, there are two singlets, two triplets, and two broken-symmetry configurations. The broken-symmetry configurations can linearly combine and form a singlet and a triplet. The true singlet wave functions can be obtained through configuration interaction of the singlet configurations.

Under an orbital transformation, for example, the following one,

$$|A\rangle = \frac{|a\rangle + |b\rangle}{\sqrt{2}} \tag{3a}$$

$$|B\rangle = \frac{|a\rangle - |b\rangle}{\sqrt{2}} \tag{3b}$$

the three component terms become

$$\Phi_1 = \frac{|A\bar{A}\rangle + |B\bar{B}\rangle}{\sqrt{2}} \tag{4a}$$

$$\Phi_2 = \frac{|A\bar{B}\rangle - |\bar{A}B\rangle}{\sqrt{2}} \tag{4b}$$

$$\Phi_3 = \frac{|A\bar{A}\rangle - |B\bar{B}\rangle}{\sqrt{2}} \tag{4c}$$

The form of the first term is unchanged and so are the triplet terms not shown here. This holds true for general unitary transformations. These transformed orbitals are useful for understanding and analyzing results in specific systems, although these orbitals do not necessarily diagonalize any one-electron Hamiltonian and cannot be assigned orbital energies from eigenvalues.

Usually, the most interesting states to chemists are the three triplet states and the one low-lying singlet states. This singlet state can be either a closed-shell singlet (for example, methylene[5]), or possibly be an open-shell singlet (for example, cyclobutadiene). The energy difference between the triplets and the low-lying singlet differs from species to species, and can be used to predict the electronic properties and chemical reactivities of a given diradical.

Despite the long history of diradical problems,[2,6−8] it still remains a hot topic to pursue a theoretical method that can efficiently and accurately describe a diradical system, especially its open-shell singlet state. Because of the energy near-degeneracy of the orbitals that diagonalize the one-body effective Hamiltonian, the open-shell singlet state has strong static correlation. In other words, the state has a strong multiconfiguration nature, and in order for it to be theoretically well described, multireference methods are required. The commonly used multireference wave function methods include the complete active space self-consistent-field (CASSCF) and its second order perturbative treatment (CASPT2),[9] the multireference configuration interaction (MR-CI),[10] and the multireference coupled cluster theory (MR-CC).[11,12] These methods are generally accurate. However, they are computationally demanding and therefore limited to relatively small systems. Another category of methods that are commonly used is usually called the broken-symmetry (BS) approach.[13−16] In this approach, instead of directly describing the challenging open-shell singlet state, one uses unrestricted density functional theory (UDFT) or unrestricted coupled cluster theory (UCC) to describe one of the broken-symmetry states (Figure 1), which is roughly a half open-shell singlet contaminated by a half triplet state and energetically lies approximately half way in between the triplets and the open-shell singlet state. The amount of spin-contamination can be further corrected by spin-projection.[17,18] Despite its low cost and great popularity, the broken-symmetry approach is an indirect method of obtaining the open-shell singlet, whose SCF calculation only targets on the spin-contaminated BS state; moreover, the spin projected DFT is also reported to lead to degraded potential energy surfaces.[19]

In the past few years, some new methods were developed and showed their strength in describing diradical systems. One of them is the fractional-spin method[20] or the variational fractional-spin method.[21] They are able to directly obtain the open-shell singlet state without spin contamination using a fractionally occupied state. This category of methods is the fractional-spin version of delta-SCF approach,[13,22] and it can obtain good singlet−triplet (ST) gaps (E_S−E_T) for many types of diradicals;[20,21] however, because of the limitations of current density functional approximations (DFAs), the (variational) fraction-spin method suffers from DFA's intrinsic static correlation error[23,24] and therefore cannot well describe diradicals with disjoint features.[21] Another category of new methods uses the concept of spin flip.[25,26] These methods include spin-flip equation-of-motion coupled cluster theory (SF-EOM-CC),[27−29] spin-flip configuration interaction (SF-CI),[30,31] restricted active space spin-flip configuration interaction (RAS-SF-CI)[32,33] and spin-flip time-dependent density

DOI: 10.1021/jp512727a
J. Phys. Chem. A 2015, 119, 4923−4932

functional theory (SF-TDDFT) with either collinear[34] or noncollinear kernel.[35−37] These spin-flip methods start with an open-shell high-spin triplet and obtain singlet states through spin-flip excitation operators. With an unrestricted initial reference, these spin-flip methods can obtain improved results over the BS approach for diradicals[31,32,34,38−41] with a tolerably small amount of spin contamination. Among these methods, SF-CIS and SF-TDDFT are able to achieve low $O(r^4)$ scaling, which makes them applicable to large systems. The introduction of noncollinear kernel[35−37] improved the original collinear SF-TDDFT, although at the cost of being more functional sensitive.[42] With a restricted open-shell calculation and by applying spin-adapted operators and the tensor reference, one can formulate spin-pure and spin-complete SF-TDDFT.[43−45]

Recently, we employed the pairing matrix fluctuation[46] or the time-dependent density functional theory with pairing field (TDDFT-P)[47] to solve excitation problems. Results show that even the first-order approximation, particle−particle random phase approximation (pp-RPA), can well describe single, double, charge transfer, and Rydberg excitations.[46,48] It is also shown by Zhang et al. that pp-RPA is able to perform geometry optimization for excited states as well as the ground state, and it is also able to describe single-bond breaking.[49] The higher-order approximation of pp-RPA with an additional particle−hole excitation was also tested on some small systems.[50] In this paper, we will treat the ST gaps in diradical systems as an excitation problem and apply pp-RPA to this challenging problem. We will use several well studied molecules to show the generally good performance of pp-RPA. This paper is organized as follows. In the Methods section, we briefly review the theory of pp-RPA for calculating excitation energies and discuss its ability to solve diradical problems. Then we present the Results and Discussions. Finally we give our Conclusion.

METHODS

The pp-RPA excitation formula can be derived in many ways. The equation-of-motion formalism[51,52] is an easy starting point and it justifies the use of Hartree−Fock (HF) references. Through pairing matrix fluctuation[46,53,54] or the TDDFT-P theory,[47] the use of DFT references can be introduced and well justified. In this paper, we will not rederive the pp-RPA equation. For readers who are interested in the theory, please refer to refs 46, 47, and 51−54.

The pp-RPA working equation takes the following form,

$$\begin{bmatrix} \mathbf{A} & \mathbf{B} \\ \mathbf{B}^{\dagger} & \mathbf{C} \end{bmatrix} \begin{bmatrix} \mathbf{X} \\ \mathbf{Y} \end{bmatrix} = \omega \begin{bmatrix} \mathbf{I} & \mathbf{0} \\ \mathbf{0} & -I \end{bmatrix} \begin{bmatrix} \mathbf{X} \\ \mathbf{Y} \end{bmatrix} \tag{5}$$

with the matrix elements

$$A_{ab,cd} = \delta_{ac}\delta_{bd}(\epsilon_a + \epsilon_b) + \langle ab||cd\rangle \tag{6a}$$

$$B_{ab,ij} = \langle ab||ij\rangle \tag{6b}$$

$$C_{ij,kl} = -\delta_{ik}\delta_{jl}(\epsilon_i + \epsilon_j) + \langle ij||kl\rangle \tag{6c}$$

The definition of two-electron integrals is

$$\langle pq||rs\rangle \equiv \langle pq|rs\rangle - \langle pq|sr\rangle \tag{7}$$

and

$$\langle pq|rs\rangle \equiv \int d\mathbf{x}\, d\mathbf{x}' \frac{\phi_p^*(\mathbf{x})\, \phi_q^*(\mathbf{x}')\, \phi_r(\mathbf{x})\, \phi_s(\mathbf{x}')}{|\mathbf{r} - \mathbf{r}'|} \tag{8}$$

In this paper, we adopt the convention that *a,b,c,d* are for unoccupied molecular orbitals, *i,j,k,l* for occupied orbitals, and *p,q,r,s* for general orbitals. The eigenvalues ω's can represent two-electron addition energies if the normalization sign of the corresponding eigenvector is positive or two-electron removal energies if the normalization sign is negative.

Starting from an $(N-2)$-electron (two-electron deficient) reference, through the two-electron addition process, the system can reach a series of its N-electron states (neutral states), including both the ground state and excited states. The eigenvalues in eq 5 represent the transition energy from the $(N-2)$-reference to the final neutral states. Then if we subtract two transition energies, the difference will be the energy gap between the two involved neutral states. Specifically, if one neutral state is the ground state $|0,N\rangle$, and the other is an excited state $|n,N\rangle$, then the energy difference is the excitation energy,

$$E_n^N - E_0^N = (E_n^N - E_{\text{ref}}^{N-2}) - (E_0^N - E_{\text{ref}}^{N-2}) = \omega_n - \omega_0 \tag{9}$$

It is worth noting that in wave function theory, the double electron-attachment equation-of-motion coupled cluster theory (DEA-EOM-CC)[55,56] has also been applied to excitation problems with the same philosophy. The difference is that pp-RPA can use DFT to describe the $(N-2)$-electron system, and the employment of single-determinant references makes it computationally more practical to large systems. Through direct diagonalization, the whole excitation spectrum can be obtained with an $O(r^6)$ scaling, where r is the number of occupied orbitals, or the number of virtual ones, depending on which number is larger. However, an iterative Davidson method with a lower $O(r^4)$ scaling can be implemented to capture the lowest few excitations.[48]

In a diradical system, when we remove the two nonbonding electrons, the remaining $(N-2)$-electron system is usually a well-behaved closed-shell singlet species without dramatic static correlation. Therefore, the $(N-2)$-electron reference can be well described by some well-known density functionals, such as B3LYP[57,58] or PBE.[59] In contrast, the two nonbonding electrons, which dominate the chemical behavior of a diradical, show strong static correlation and need more accurate multireference descriptions, such as CASSCF, CASPT2, or MR-CI. Through a seamless combination of DFT for the $(N-2)$-electron reference and a subspace CI for the two nonbonding electrons (Figure 2), the pp-RPA is expected to describe diradicals well with a low cost.

Our spin-adapted pp-RPA[60] is implemented in the local QM4D package.[61] A Davidson algorithm is used to calculate the lowest few exciations.[48] We report our results on four

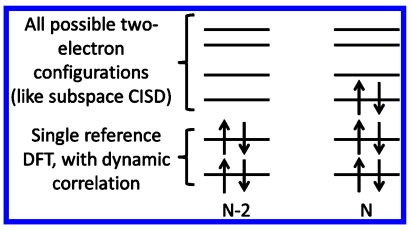

Figure 2. Pp-RPA combines DFT with wave function methods. The $(N-2)$-electron system is described by single reference DFT. The two electrons added in can form any two-electron configuration within the virtual space, resembling a subspace configuration interaction singles and doubles (CISD).

DOI: 10.1021/jp512727a
J. Phys. Chem. A 2015, 119, 4923−4932

Table 1. Adiabatic Singlet-Triplet Gaps (in kcal/mol) for Diatomic Diradicals[a]

	expt[b]	pp-HF	pp-B3LYP	pp-PBE	(V)FS-PBE[c]	SF-CIS[d]	SF-CIS(D)[d]	SF-LDA[e]
NH	35.9	30.9	38.5	40.5	41.1	40.7	37.1	35.6
OH^+	50.5	45.5	52.3	54.2	54.8	53.6	50.2	48.8
NF	34.3	28.6	28.7	28.3	34.0	40.8	35.3	30.3
O_2	22.6	23.1	23.6	23.5	26.2	33.4	24.6	23.7
MAE		4.1	2.8	3.8	3.4	6.3	1.1	1.8

[a]The geometries for pp-RPA calculations are adopted from ref 20. Aug-cc-pVDZ basis set is used for all pp-RPA calculations. The adiabatic gap correction is based on eq 10a. [b]Experimental values from ref 63. [c](Variational) fractional-spin results from ref 21 with 6-311++G(2d,2p) basis set. [d]Spin-flip CI results from ref 38 with cc-pVQZ basis set. [e]Spin-flip TDLDA with noncollinear kernel results from ref 36 with TZ2P basis set.

Table 2. Adiabatic Singlet−Triplet Gaps (in kcal/mol) for Carbene-like Diradicals[a]

		ref 1[b]	ref 2[c]	pp-HF	pp-B3LYP	pp-PBE	(V)FS-PBE[d]	SF-CIS[f]	SF-CIS(D)[f]	SF-LDA[g]	SF-PBE[g]	SF-B3LYP[i]
CH_2	$^1A_1$	9.0	9.7	−2.4	3.7	5.9	15.7	20.4	14.1	11.8	12.3	0.4
	$^1B_1$	31.7	32.5	26.3	32.0	33.5	36.2	43.2	38.0	30.7	32.3	23.2
	2^1A_1			58.3	45.6	52.9	54.8	*e*	83.0	68.1	61.7	64.9	46.1
NH_2^+	$^1A_1$	29.0	28.9	12.8	23.1	25.7	35.5	38.6	30.9	29.6	31.3	17.3
	$^1B_1$	43.6	43.0	36.5	42.0	43.7	47.8	49.6	45.2	40.8	43.3	31.8
	2^1A_1			76.5	62.3	70.2	72.5	*e*	100.9	83.8	81.2	86.1	62.9
SiH_2	$^1A_1$	−21.0	−20.6	−24.9	−28.7	−28.3	−16.1	−11.6	−17.9	−21.5	−22.2	−30.1
	$^1B_1$	23.5	24.1	24.0	26.3	26.4	24.0	39.2	31.0	19.0	20.3	16.3
	2^1A_1			57.0	51.7	54.0	52.7	*e*	79.4	70.9	52.4	56.2	46.6
PH_2^+	$^1A_1$	−17.0	−18.3	−25.2	−24.6	−23.5	−12.8	−8.9	−15.7	−19.3	−19.0	−29.2
	$^1B_1$	27.0	27.6	28.9	30.1	30.2	28.8	41.0	33.5	22.4	24.5	18.4
	2^1A_1			65.6	60.6	61.1	59.9	*e*	95.8	76.9	58.8	64.6	51.5
MAE1[h]					6.8	4.3	3.5	4.2	10.7	4.2	2.4	1.9	9.7
MAE2[i]					7.6	4.3	3.7		15.5	6.2	3.2	2.7	10.8

[a]The geometries for pp-RPA calculations are adopted from ref 38. Aug-cc-pVDZ basis set is used for all pp-RPA calculations. The adiabatic gap correction is based on eq 10a. [b]Experimental values for CH_2 from ref 70. MR-CI values for NH_2^+ from ref 71. Experimental values for SiH_2 from refs 72 and 73. Experimental values for PH_2^+ from ref 74. [c]EOM-SF-CCSD(dT)/aug-cc-pVQZ results from ref 42. [d](Variational) fractional-spin results from ref 21 with 6-311++G(2d,2p) basis set. [e](Variational) fractional-spin methods are not able to capture the 2^1A_1 state. [f]Spin-flip CI results from ref 38 with TZ2P basis set. [g]Spin-flip TDDFT with noncollinear kernel results from ref 42 with cc-pVTZ basis set. [h]Due to limited data in ref 1, 2^1A_1 data are not counted in when MAE is calculated. [i]All excitation values are taken into account when comparing with data from ref 2. Error for (V)FS-PBE is not calculated because of the lack of 2^1A_1 data.

diatomic diradicals (NH, OH^+, NF, O_2), four carbene-like diradicals (CH_2, NH_2^+, SiH_2, PH_2^+), three disjoint diradicals (·$CH_2CH_2CH_2$·, ·$CH_2CH_2CH_2CH_2CH_2CH_2$·, ·$CH_2CH_2CH_2$-$CH_2CH_2C(CH_3)H$·), two four-electron diradicals (cyclobutadiene (C_4H_4) and TMM ($C(CH_2)_3$)), and three benzyenes (*o*-, *m*-, *p*-). The optimized geometries are adopted from their original references and summarized in the Supporting Information.[62] ST gaps for these diradicals are calculated through pp-RPA with HF, B3LYP, and PBE functionals, which include different percentages of HF exchange. The aug-cc-pVDZ basis set, which has been shown in our previous paper[48] to give converged excitation energies, is adopted in all pp-RPA calculations. Vertical ST gaps Eg_v are directly calculated with eq 9, while adiabatic gaps Eg_a are calculated from Eg_v, plus a correction on the potential energy curves obtained from SCF calculations for the *N*-electron system. Two flavors of correction can be employed, either on the triplet energy curve 10a or on the singlet energy curve 10b, depending on which *N*-electron spin state can be better described by the functional used.

$$Eg_a = E_{S,Sgeo} - E_{T,Tgeo} = Eg_{v,Sgeo} + (E_{T,Sgeo} - E_{T,Tgeo}) \quad (10a)$$

$$Eg_a = E_{S,Sgeo} - E_{T,Tgeo} = Eg_{v,Tgeo} + (E_{S,Sgeo} - E_{S,Tgeo}) \quad (10b)$$

In most cases, the *N*-electron triplet state is better described by single reference methods. Therefore, the correction based on eq 10a is adopted unless specifically specified.

RESULTS AND DISCUSSIONS

Diatomic Diradicals. The test set of diatomic diradicals are adopted from a previous fractional-spin study.[20] This set of diradicals was also well investigated and benchmarked earlier by spin-flip methods.[36,38] There are four diradicals in this set: NH, OH^+, NF, and O_2, which are two pairs of isoelectronic species. Although their geometries are simple and characterized by a single bond length, their electronic structures are nontrivial. For these diradicals, the configuration Φ_2 and Φ_3 in eq 2a and 3a span a degenerate irreducible representation, generating a 2-fold degenerate singlet $^1\Delta$ state. The triplet $^3\Sigma$ state is below the $^1\Delta$ state, while the singlet $^1\Sigma$ state is above it. The calculated singlet−triplet ($^1\Delta$−$^3\Sigma$) gaps are summarized in Table 1. Overall, there is a good agreement between pp-RPA calculations and experimental results. With the aug-cc-pVDZ basis set, the pp-RPA with HF reference (pp-RPA-HF, or pp-HF for short), which has no dynamic correlations for the (N − 2)-reference, also performs well for these small molecules with a small underestimation of the ST gaps. The pp-RPA with DFT references performs better and the mean absolute error for pp-RPA-B3LYP is as small as 2.8 kcal/mol. These pp-RPA results are better than SF-CIS (MAE 6.3 kcal/mol) and comparable

DOI: 10.1021/jp512727a
J. Phys. Chem. A 2015, 119, 4923−4932

Table 3. Vertical Singlet−Triplet Gaps (in kcal/mol) for Disjoint Diradicals[a]

		ref[b]	pp-HF	pp-B3LYP	pp-PBE	(V)FS-PBE[c]	SF-LDA[d]	SF-PBE[d]	SF-B3LYP[d]	SF-ωPBEh[d]
$\cdot CH_2CH_2CH_2\cdot$		1.8	2.4	4.4	5.4	20.4				
$\cdot CH_2(CH_2)_4CH_2\cdot$	$^1A_1$	0.0	0.0	0.1	0.1		0.0	0.0	0.0	0.0
	$^1B_1$	160.8	79.9	147.4	159.2		35.1	38.2	67.8	133.2
	2^1A_1	163.1	80.6	149.0	161.9		35.2	38.3	67.9	133.6
$\cdot CH_2(CH_2)_4C(CH_3)H\cdot$	$^1A_1$	−0.2	−0.3	0.1	0.4		−1.5	−1.2	−1.1	−0.6
	2^1A_1	131.1	66.1	129.0	139.8		26.9	23.2	54.8	113.3
	3^1A_1	144.3	78.3	142.1	152.3		46.4	44.6	74.5	127.6

[a]For pp-RPA calculations, the geometry of $\cdot CH_2CH_2CH_2\cdot$ is adopted from ref 21, and the geometries of $\cdot CH_2(CH_2)_4CH_2\cdot$ and $\cdot CH_2(CH_2)_4C(CH_3)H\cdot$ are adopted from ref 42. Aug-cc-pVDZ basis set is used for all pp-RPA calculations. [b]CASPT2(2,4)/6-311++G(2d,2p) result for $\cdot CH_2CH_2CH_2\cdot$ from ref 21. EOM-SF-CCSD(dT)/6-311G(d) results for $\cdot CH_2(CH_2)_4CH_2\cdot$ and $\cdot CH_2(CH_2)_4C(CH_3)H\cdot$ from ref 42. [c](Variational) fractional-spin result from ref 21 with 6-311++G(2d,2p) basis set. [d]SF-TDDFT with noncollinear kernel results from ref 42 with cc-pVTZ basis set.

with (V)FS-PBE (MAE 3.4 kcal/mol). However, SF-CIS(D)/cc-pVDZ and SF-TDLDA/TZ2P with noncollinear kernel (NC-SF-TDLDA) have mean absolute error even below 2 kcal/mol, which shows their good performances in these very small diradicals.

Carbene-like Diradicals. Carbene and carbene-like diradicals are important species that are widely used in organic chemistry.[3] Here we choose a well-studied set[20,21,38,42] for testing purposes. This set includes CH_2, NH_2^+, SiH_2, and PH_2^+, which are also two pairs of isoelectronic molecules. Unlike the previous diatomic diradicals, carbene-like diradicals have nondegenerate frontier orbitals—one σ orbital and one π orbital—with different symmetry, which means the open-shell singlet ($\sigma^1\pi^1$) and closed-shell singlet (σ^2 or π^2) cannot further mix through configuration interaction. Take methylene as an example. The lowest state is triplet $^3B_1$ with one electron occupying σ and another one occupying π. Then the closed-shell singlet $^1A_1$ comes next with mostly the σ orbital doubly occupied and a small contribution from π orbital doubly occupied. The open-shell singlet $^1B_1$ with singly occupied σ and π is the third state and finally there is another closed-shell $^1A_1$ which is mostly the π orbital doubly occupied. Despite the relatively simple orbital picture, the energy alignment might change greatly depending on the center atom and the surrounding environments. For example, in PH_2^+ and SiH_2, the order of $^3B_1$ and the first $^1A_1$ is switched compared to CH_2 and NH_2^+, resulting in a negative ST gap; Chen et al.[5] also have theoretically attempted to lower the energy of the π-doubly occupied $^1A_1$ state to make it the ground state by a proper choice of ligand groups.

The pp-RPA results for these carbene-like diradicals are summarized in Table 2. For methylene, the first adiabatic ST gap historically[64,65] had been a puzzle, in which the value was finally agreed by experiments and calculations to be as small as only 9 kcal/mol.[66,67] The pp-RPA with B3LYP and PBE references reasonably predicts the adiabatic gap to be 3.7 and 5.9 kcal/mol, respectively. For the HF reference, the gap is predicted to be negative (−2.4 kcal/mol), which shows that here the HF reference is not as good as DFT references. The (variational) fractional-spin method overestimates the gap (15.7 kcal/mol) and so do SF-CI (20.4 kcal/mol) and SF-CIS(D) (14.1 kcal/mol). The SF-TDDFT with noncollinear kernels greatly depends on functionals, with the hybrid B3LYP functional greatly underestimating the gap, while the local LDA and PBE functional well predict the gap. For the next gap between $^3B_1$ and $^1B_1$ states, the result of pp-RPA with DFT references (32.0 kcal/mol for B3LYP and 33.5 kcal/mol for PBE), together with SF-TDLDA (30.7 kcal/mol) and SF-TDPBE (32.3 kcal/mol), is even closer to the reference value (31.7 kcal/mol) than that of SF-CIS(D) (38.0 kcal/mol). SF-CIS and SF-B3LYP still have large systematic errors. The gap between $^3B_1$ and the second $1A^1$ is similar, with pp-PBE and SF-TDLDA performing the best.

It is also worth noting that many existing works[67−69] show that at the optimized singlet geometry for methylene, the singlet energy is very close to or even lower than the triplet energy. Therefore, a very small or negative vertical gap is expected. With pp-RPA, we also observed this phenomenon, with −7.3 and −4.5 kcal/mol vertical ST gap obtained with B3LYP and PBE references, respectively (see Supporting Information[62] for detailed data).

For other carbene-like molecules, the results are similar to methylene. Interestingly, the pp-RPA results with B3LYP reference—more HF exchange than PBE and less HF exchange than HF—mostly lie between the results with PBE and those with HF references. This phenomenon implies that the amount of HF exchange and its related virtual orbital energy alignments may play an important role in achieving good accuracy. Overall, for this test set, pp-RPA with DFT references—with no or a small amount of HF exchange—perform well with 4.3 kcal/mol MAE for the B3LYP reference and 3.5 or 3.7 kal/mol for the PBE reference. Although they are still not as good as SF-TDLDA (2.4 or 3.2 kcal/mol) and SF-TDPBE (1.9 or 2.7 kcal/mol), they are much better than SF-CIS (10.7 or 15.5 kcal/mol) and SF-TDB3LYP (9.7 or 10.8 kcal/mol), and similar to or slightly better than (V)FS-PBE (4.2 kcal/mol) and SF-CIS(D) (4.2 or 6.2 kcal/mol).

Disjoint Diradicals. Disjoint diradicals are problematic for the (variational) fractional-spin method because of the static correlation error intrinsic to commonly used DFAs.[21,23,24] For $\cdot CH_2CH_2CH_2\cdot$, the reference vertical ST gap is 1.8 kcal/mol. Fractional-spin LDA (12.8 kcal/mol) and fractional-spin PBE (20.4 kcal/mol) greatly overestimate the gaps.[21] In contrast, pp-RPA with DFT references give a reasonably small gap, with 4.4 and 5.4 kcal/mol for B3LYP and PBE, respectively (Table 3). The pp-RPA-HF also reasonably predicts a vertical gap of 2.4 kcal/mol. The advantage of pp-RPA is even more clear for two longer disjoint diradicals, that is, $\cdot CH_2(CH_2)_4CH_2\cdot$ and $\cdot CH_2(CH_2)_4C(CH_3)H\cdot$. The pp-RPA with DFT references cannot only well describe the lowest singlet−triplet gap, but also well predict the higher excitations with charge transfer character.

These disjoint diradicals can be viewed as two electrons connected by a $(CH_2)_n$ bridge. If we ignore the bridge, the systems resemble the stretched H_2 molecule. It is well-known that the stretched H_2 has strong static correlation, and most

DOI: 10.1021/jp512727a
J. Phys. Chem. A 2015, 119, 4923−4932

Table 4. Singlet−Triplet Gaps[a] (in kcal/mol) for Four-π-Electron Diradicals[b]

		ref 1[c]	ref 2[d]	pp-HF	pp-B3LYP	pp-PBE	(V)FS-PBE[e]	SF-CIS[f]	SF-CIS(D)[f]	SF-LDA[g]	SF-PBE[g]	SF-B3LYP[g]	SF-ωPBEh[g]
TMM	$^1B_1$	16.7	16.0	17.1	16.3	15.6	21.5	23.5	23.6	15.6	17.2	17.0	16.4
	$^1A_1$	19.1	19.5	26.4	33.9	35.5		20.4	20.6	13.0	13.3	15.9	18.8
	2^1A_1		79.5	76.6	107.3	114.4		151.7	82.3	30.5	33.9	46.6	68.7
cyclobutadiene		−8.1	7.2	6.7	6.5	16.5							

[a]Adiabatic gaps for TMM (correction based on eq 10a) and vertical gaps for square cyclobutadiene. [b]For pp-RPA calculations, the geometry of TMM and Cyclobutadiene are adopted from refs 38 and16, respectively. Aug-cc-pVDZ basis set is used for all pp-RPA calculations. [c]MCQDPT2(10,10)/cc-pVTZ results for TMM from ref 38. CASSCF/MkCCSD result for cyclobutadiene from ref 16. [d]EOM-SF-CCSD(dT)/6-311G(d) results from ref 42. [e](Variational) fractional-spin results from ref 21 with 6-311++G(2d,2p) basis set. [f]Spin-flip CI results from ref 38 with cc-pVQZ basis set. [g]SF-TDDFT with noncollinear kernel results from ref 42 with cc-pVTZ basis set.

single reference methods will fail to describe the stretching process.[24] Meanwhile, it is also a challenge for DFAs to describe the charge transfer excitation in stretched H_2 because of common DFAs' large delocalization error. Similarly, with an additional $(CH_2)_n$ bridge, these long disjoint diradicals become even more challenging. Fortunately, the subspace CISD treatment frees pp-RPA from static correlation and enables it to well describe the lowest $^3A_1$ and $^1A_1$ states. The full coulomb kernel enables pp-RPA to correctly capture the asymptotic behavior of charge-transfer excitations.[46] For spin-flip TDDFT, the employment of high spin references and spin-flip excitation operators also frees it from static correlation error, thus the $^1A_1$−$^3A_1$ gap is well described by all functionals. However, when it comes to excitations, the erroneous DFA kernels in SF-TDDFT account for the greatly underestimated charge transfer excitations. Only when the long-range corrected functional (for example, ωPBEh) is employed can the problem be relieved.

Four-Electron Diradicals. Diradicals with four π electrons also have a long history. They were discussed in detail in Borden and Davidson's work.[75] The non-Kekule molecule trimethylenemethane (TMM) is one of the examples.[76−82] In a single reference picture, TMM has four electrons occupying four π atomic orbitals. If there is D_{3h} geometry, these four π orbitals form one molecular orbital lying at the bottom, one at the top and two degenerate ones in the middle. Therefore, two electrons form a pair and occupy the lowest molecular orbital and two remaining electrons occupy the two degenerate orbitals, forming a diradical. A further mix of open-shell and closed-shell singlet determinants is allowed with D_{3h} geometry because of the proper symmetry of the degenerate orbitals. Therefore, the picture is much like the diatomic cases. According to Hund's rule, which is obeyed in this case, the triplets show lower energy than the singlets. When the D_{3h} symmetry is not preserved, the state degeneracy is broken. One state finds its global minimum at a twisted nonplanar geometry, and this state is assigned the symbol $^1B_1$. The other state has a local minimum with the restricted planar geometry, and it is assigned as the $^1A_1$ state.[77] The calculated adiabatic ST gaps for TMM are summarized in Table 4. It can be seen that the lowest adiabatic ST gap ($^1B_1$−$^3A_2'$) is well predicted by pp-RPA with errors even less than 1 kcal/mol. However, for the second ST gap ($^1A_1$−$^3A_2'$), the pp-RPA greatly overestimates the results. This overestimation is very likely to be related to the two bonding electrons treated with DFT. Even though in a single-reference picture these two electrons form a pair and occupy a b_1 orbital that seems to play a less important role in determining the chemical properties of the diradical, this b_1 orbital is very sensitive to the chemical environment at the optimized $^1A_1$ geometry. With a restricted B3LYP SCF calculation for the singlet neutral system, in which the four electrons line up as $1b_1^2\,1a_2^2$, the b_1 orbital mostly localizes as a π bond between the central atom and the closest carbon atom (Figure 3a). However, a calculation for the $(N-2)$-electron

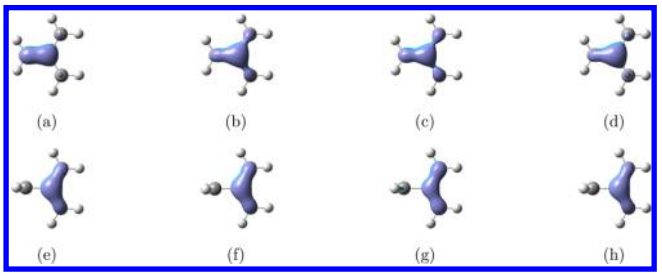

Figure 3. Orbital picture of the b_1 orbital occupied by the two bonding π electrons calculated with the B3LYP functional: (a) neutral singlet calculation at optimized $^1A_1$ geometry; (b) $(N-2)$-electron singlet calculation at optimized $^1A_1$ geometry; (c) neutral triplet calculation (alpha orbital) at optimized $^1A_1$ geometry; (d) neutral triplet calculation (beta orbital) at optimized $^1A_1$ geometry; (e) neutral singlet calculation at optimized $^1B_1$ geometry; (f) $(N-2)$-electron singlet calculation at optimized $^1B_1$ geometry; (g) neutral triplet calculation (alpha orbital) at optimized $^1B_1$ geometry; (h) neutral triplet calculation (beta orbital) at optimized $^1B_1$ geometry.

reference shows it to be much more diffuse onto the other two farther carbon atoms (Figure 3b). An unrestricted triplet calculation for the neutral system gives pictures between these two cases (Figure 3 orbitals c and d). Overall, from the most localized one to the most diffuse one, the order is neutral singlet orbital, neutral triplet beta orbital, neutral triplet alpha orbital, and finally the $(N-2)$-electron singlet orbital. The frozen b_1 orbital for the $(N-2)$-electron reference might be too diffuse compared to the real picture, making the $(N-2)$-electron core not well described. This inaccurate description of the core leads to the large error. Interestingly, in contrast, this b_1 orbital is not quite sensitive to the chemical environment at the optimized $^1B_1$ geometry (Figure 3 orbitals e−h). Therefore, the frozen core should be close to the real picture and the vertical gap ($^1B_1$−$^3A_2'$) at the optimized $^1B_1$ is well described, finally making the adiabatic gap also well predicted by pp-RPA.

Spin-flip TDDFT with LDA, PBE, and B3LYP functionals can also well predict the lowest $^1B_1$−$^3A_2'$ gap. However, they greatly underestimate the two higher $^1A_1$−$^3A_2'$ gaps. Unlike pp-RPA, SF-TDDFT can correlate the lower non-HOMO excitation configurations, and therefore the error for SF-TDDFT mostly lies in the functional that is employed. When the long-range corrected functional ωPBEh with a larger portion of Hartree−Fock exchange is employed, the error gets smaller.

Another typical four-π-electron system is cyclobutadiene.[27,29,83−89] It has similar single-reference orbital picture

DOI: 10.1021/jp512727a
J. Phys. Chem. A 2015, 119, 4923−4932

Table 5. Adiabatic Singlet−Triplet Gaps (in kcal/mol) for Benzynes[a]

	expt[b]	pp-HF	pp-B3LYP	pp-PBE	SF-CIS[c]	SF-CI(D)[c]	SF-LDA[d]	SF-PBE[d]	SF-B3LYP[d]	SF-ωPBEh[d]
o-	−37.5	−45.6	−37.4	*e*	−23.2	−35.7	−47.5	−44.3	−46.9	−43.6
m-	−21.0	−35.5	−22.1	*e*	−3.82	−19.4	−29.0	−27.7	−26.1	−20.8
p-	−3.8	−4.0	−0.6	−8.9	−0.32	−2.1	−10.5	−9.6	−6.9	−4.1

[a]The *o*- and *m*- benzyne geometries for pp-RPA calculations are adopted from ref 38; however, the *p*-benzyne geometry is adopted form ref 42 optimized by SF-CCSD method, which gives better optimized structure in terms of DFT total energy. Aug-cc-pVDZ basis set is used for all pp-RPA calculations. The adiabatic gap correction is based on eq 10b. [b]Experimental values from ref 94. [c]Spin-flip CI results from ref 38 with cc-pVQZ basis set. [d]SF-TDDFT with noncollinear kernel results from ref 42 with cc-pVTZ basis set. [e]No results for PBE reference because of an SCF convergence failure for the $(N-2)$-electron system.

to TMM. However, this molecule violates the Hund's rule—the open-shell singlet is lower in energy than the triplets, even though the single-reference frontier orbitals are degenerate. This is even true for the vertical gap of the square cyclobutadiene.[90] This phenomenon is related to the D_{4h} symmetry and its Φ_2 and Φ_3 are not degenerate and are of different symmetry. A pictorial explanation is given by Borden and Davidson[75] by considering the molecule's D_{4h} symmetry and the possibility to localize degenerate MOs. The reference vertical ST gap for square cyclobutadiene is negative (−8.1 kcal/mol). Unfortunately, although much better than the fractional-spin method (16.5 kcal/mol), pp-RPA also predicts positive ST gaps (6.5−7.5 kcal/mol) whatever reference is used. This also may be related to the inaccurate frozen description of the two bonding π electrons, which should be described with more explicit correlation together with the two nonbonding electrons.

Benzynes. Benzyne has three isomers (*o*-, *m*-, *p*-). These isomers all have closed-shell singlets as the ground state, but they still hold some diradical characters with interesting chemistry behaviors that have been theoretically studied.[38,42,91−93] Following the ortho, meta, para sequence, the diradical character increases, resulting in a decrease of ST gaps. The results are summarized in Table 5. There are some problems with the convergence of $(N-2)$-electron systems with the PBE functional. Therefore, some PBE data are missing. Apart from that, the pp-RPA-DFT results are in good agreement with experimental results, especially with the B3LYP reference. The pp-RPA-B3LYP results are better than the SF-CIS and SF-TDDFT with LDA, PBE, and B3LYP functional. They are similar to SF-CIS(D) and SF-TD-ωPBEh. Here pp-RPA-HF gives results with larger errors, probably because of the lack of dynamic correlation for the relatively large-size $(N-2)$-electron reference. The good performance of pp-RPA-B3LYP on these relatively larger molecules shows that it might be promising to use pp-RPA in even larger and more complex diradical systems.

CONCLUSION

The pp-RPA describes diradical systems by starting from an SCF $(N-2)$-electron reference, and then adding two electrons with explicit correlation. The relatively simpler $(N-2)$ system can be well described by a single-determinant DFT reference, while the two electrons are described in a subspace CI fashion. The combination of DFT with correlated wave function methods, as well as the treatment of all neutral states on the same footing,[46] enables pp-RPA to describe diradicals both accurately and efficiently. The bare coulomb kernel of pp-RPA ensures a correct description of charge separated and charge transferred state. In this work, we showed the pp-RPA results with HF, B3LYP, and PBE functionals for a variety of categories of diradicals, including diatomic diradicals, carbene-like diradicals, disjoint diradicals, four-π-electron diradicals and larger benzyne diradicals. The difference between different functional references shows that the amount of HF exchange affects the final results by affecting the virtual orbital energies. As to the results, except for some states for the four-π-electron diradicals with important correlation contributions from more than the two nonbonding electrons, the pp-RPA with DFT references generally gives rise to good results, which shows that pp-RPA is much more accurate than SF-CIS. It is comparable or better than (variational) the fractional-spin method. In some small diradical systems, such as diatomic diradicals and carbene-like diradicals, the error for pp-RPA is slightly larger than that of SF-TDDFT with LDA and PBE functionals. However, when it comes to more difficult disjoint diradicals and benzynes, the pp-RPA with DFT reference performs much better, and it becomes comparable to SF-CIS(D) and SF-TDωPBEh. Moreover, the pp-RPA is an inexpensive first order theory with $O(r^4)$ scaling that is newly applied to molecular systems. Although further exploration of functionals and kernels may further improve the results and a better converging method may relieve some SCF convergence problems for the $(N-2)$ system, the pp-RPA is already now a reliable theoretical method for describing diradical systems and could be promising in solving much larger and more challenging diradical-related problems.

ASSOCIATED CONTENT

Supporting Information

Geometries, detailed calculation procedure, and detailed data. The Supporting Information is available free of charge on the ACS Publications website at DOI: 10.1021/jp512727a.

AUTHOR INFORMATION

Corresponding Author

*E-mail: Weitao.Yang@duke.edu.

Notes

The authors declare no competing financial interest.

ACKNOWLEDGMENTS

Funding support from the National Science Foundation (CHE-1362927) is greatly appreciated. We greatly thank Dr. Peng Zhang and Mr. Du Zhang for helpful discussions.

REFERENCES

(1) Salem, L.; Rowland, C. The Electronic Properties of Diradicals. *Angew. Chem., Int. Ed.* **1972**, *11*, 92−111.
(2) Abe, M. Diradicals. *Chem. Rev.* **2013**, *113*, 7011−7088.
(3) Bertrand, G. *Carbene Chemistry: From Fleeting Intermediates to Powerful Reagents*; Marcel Dekker: New York, 2002.

DOI: 10.1021/jp512727a
J. Phys. Chem. A 2015, 119, 4923−4932

(4) Morita, Y.; Suzuki, S.; Sato, K.; Takui, T. Synthetic Organic Spin Chemistry for Structurally Well-Defined Open-Shell Graphene Fragments. *Nat. Chem.* **2011**, *3*, 197−204.
(5) Chen, B.; Rogachev, A. Y.; Hrovat, D. A.; Hoffmann, R.; Borden, W. T. How to Make the $\sigma 0\pi 2$ Singlet the Ground State of Carbenes. *J. Am. Chem. Soc.* **2013**, *135*, 13954−13964.
(6) Borden, W. T.; Davidson, E. R. Singlet-Triplet Energy Separations in Some Hydrocarbon Diradicals. *Annu. Rev. Phys. Chem.* **1979**, *30*, 125−153.
(7) Davidson, E. R. In *Diradicals*; Borden, W., Ed.; Wiley: 1982; pp 73−105.
(8) Rajca, A. Organic Diradicals and Polyradicals: From Spin Coupling to Magnetism? *Chem. Rev.* **1994**, *94*, 871−893.
(9) Roos, B. O. *Advances in Chemical Physics*; John Wiley & Sons, Inc.: 2007; pp 399−445.
(10) Szalay, P. G.; Müller, T.; Gidofalvi, G.; Lischka, H.; Shepard, R. Multiconfiguration Self-Consistent Field and Multireference Configuration Interaction Methods and Applications. *Chem. Rev.* **2012**, *112*, 108−181.
(11) Evangelista, F. A.; Allen, W. D.; Schaefer, H. F. Coupling Term Derivation and General Implementation of State-Specific Multireference Coupled Cluster Theories. *J. Chem. Phys.* **2007**, *127*, 024102.
(12) Hirao, K. *Recent Advances in Multireference Methods*; World Scientific: Singapore, 1999.
(13) Ziegler, T.; Rauk, A.; Baerends, E. On the Calculation of Multiplet Energies by the Hartree-Fock-Slater Method. *Theor. Chim. Acta.* **1977**, *43*, 261−271.
(14) Noodleman, L. Valence Bond Description of Antiferromagnetic Coupling in Transition Metal Dimers. *J. Chem. Phys.* **1981**, *74*, 5737−5743.
(15) Yamaguchi, K.; Jensen, F.; Dorigo, A.; Houk, K. A Spin Correction Procedure for Unrestricted Hartree−Fock and Møller−Plesset Wavefunctions for Singlet Diradicals and Polyradicals. *Chem. Phys. Lett.* **1988**, *149*, 537−542.
(16) Saito, T.; Nishihara, S.; Yamanaka, S.; Kitagawa, Y.; Kawakami, T.; Yamada, S.; Isobe, H.; Okumura, M.; Yamaguchi, K. Symmetry and Broken Symmetry in Molecular Orbital Description of Unstable Molecules IV: Comparison between Single- and Multi-Reference Computational Results for Antiaromtic Molecules. *Theor. Chem. Acc.* **2011**, *130*, 749−763.
(17) Schlegel, H. B. Potential Energy Curves Using Unrestricted Möller−Plesset Perturbation Theory with Spin Annihilation. *J. Chem. Phys.* **1986**, *84*, 4530−4534.
(18) Chen, W.; Schlegel, H. B. Evaluation of S2 for Correlated Wave Functions and Spin Projection of Unrestricted Möller−Plesset Perturbation Theory. *J. Chem. Phys.* **1994**, *101*, 5957−5968.
(19) Wittbrodt, J. M.; Schlegel, H. B. Some Reasons Not To Use Spin Projected Density Functional Theory. *J. Chem. Phys.* **1996**, *105*, 6574−6577.
(20) Ess, D. H.; Johnson, E. R.; Hu, X.; Yang, W. Singlet-Triplet Energy Gaps for Diradicals from Fractional-Spin Density-Functional Theory. *J. Phys. Chem. A* **2011**, *115*, 76−83.
(21) Peng, D.; Hu, X.; Devarajan, D.; Ess, D. H.; Johnson, E. R.; Yang, W. Variational Fractional-Spin Density-Functional Theory for Diradicals. *J. Chem. Phys.* **2012**, *137*, 114112.
(22) Gunnarsson, O.; Lundqvist, B. I. Exchange and Correlation in Atoms, Molecules, and Solids by the Spin-Density-Functional Formalism. *Phys. Rev. B* **1976**, *13*, 4274−4298.
(23) Cohen, A. J.; Mori-Sánchez, P.; Yang, W. Insights into Current Limitations of Density Functional Theory. *Science* **2008**, *321*, 792−794.
(24) Cohen, A. J.; Mori-Sánchez, P.; Yang, W. Challenges for Density Functional Theory. *Chem. Rev.* **2012**, *112*, 289−320.
(25) Krylov, A. I. Size-Consistent Wave Functions for Bond-Breaking: The Equation-of-Motion Spin-Flip Model. *Chem. Phys. Lett.* **2001**, *338*, 375−384.
(26) Krylov, A. I. Spin-Flip Equation-of-Motion Coupled-Cluster Electronic Structure Method for a Description of Excited States, Bond Breaking, Diradicals, and Triradicals. *Acc. Chem. Res.* **2006**, *39*, 83−91.
(27) Levchenko, S. V.; Krylov, A. I. Equation-of-Motion Spin-Flip Coupled-Cluster Model with Single and Double Substitutions: Theory and Application to Cyclobutadiene. *J. Chem. Phys.* **2004**, *120*, 175−185.
(28) Slipchenko, L. V.; Krylov, A. I. Spin-Conserving and Spin-Flipping Equation-of-Motion Coupled-Cluster Method with Triple Excitations. *J. Chem. Phys.* **2005**, *123*, 084107.
(29) Manohar, P. U.; Krylov, A. I. A Noniterative Perturbative Triples Correction for the Spin-Flipping and Spin-Conserving Equation-of-Motion Coupled-Cluster Methods with Single and Double Substitutions. *J. Chem. Phys.* **2008**, *129*, 194105.
(30) Krylov, A. I. Spin-Flip Configuration Interaction: An Electronic Structure Model That Is Both Variational and Size-Consistent. *Chem. Phys. Lett.* **2001**, *350*, 522−530.
(31) Krylov, A. I.; Sherrill, C. D. Perturbative Corrections to the Equation-of-Motion Spin-Flip Self-Consistent Field Model: Application to Bond-Breaking and Equilibrium Properties of Diradicals. *J. Chem. Phys.* **2002**, *116*, 3194−3203.
(32) Casanova, D.; Head-Gordon, M. Restricted Active Space Spin-Flip Configuration Interaction Approach: Theory, Implementation and Examples. *Phys. Chem. Chem. Phys.* **2009**, *11*, 9779−9790.
(33) Zimmerman, P. M.; Bell, F.; Goldey, M.; Bell, A. T.; Head-Gordon, M. Restricted Active Space Spin-Flip Configuration Interaction: Theory and Examples for Multiple Spin Flips with Odd Numbers of Electrons. *J. Chem. Phys.* **2012**, *137*, 164110.
(34) Shao, Y.; Head-Gordon, M.; Krylov, A. I. The Spin-Flip Approach within Time-Dependent Density Functional Theory: Theory and Applications to Diradicals. *J. Chem. Phys.* **2003**, *118*, 4807−4818.
(35) Wang, F.; Ziegler, T. Time-Dependent Density Functional Theory Based on a Noncollinear Formulation of the Exchange-Correlation Potential. *J. Chem. Phys.* **2004**, *121*, 12191−12196.
(36) Wang, F.; Ziegler, T. The Performance of Time-Dependent Density Functional Theory Based on a Noncollinear Exchange-Correlation Potential in the Calculations of Excitation Energies. *J. Chem. Phys.* **2005**, *122*, 074109.
(37) Wang, F.; Ziegler, T. Use of Noncollinear Exchange-Correlation Potentials in Multiplet Resolutions by Time-Dependent Density Functional Theory. *Int. J. Quantum Chem.* **2006**, *106*, 2545−2550.
(38) Slipchenko, L. V.; Krylov, A. I. Singlet-Triplet Gaps in Diradicals by the Spin-Flip Approach: A Benchmark Study. *J. Chem. Phys.* **2002**, *117*, 4694−4708.
(39) Rinkevicius, Z.; Ågren, H. Spin-Flip Time Dependent Density Functional Theory for Singlet-Triplet Splittings in σ,σ-Biradicals. *Chem. Phys. Lett.* **2010**, *491*, 132−135.
(40) Huix-Rotllant, M.; Natarajan, B.; Ipatov, A.; Muhavini Wawire, C.; Deutsch, T.; Casida, M. E. Assessment of Noncollinear Spin-Flip Tamm-Dancoff Approximation Time-Dependent Density-Functional Theory for the Photochemical Ring-Opening of Oxirane. *Phys. Chem. Chem. Phys.* **2010**, *12*, 12811−12825.
(41) Li, Z.; Liu, W. Theoretical and Numerical Assessments of Spin-Flip Time-Dependent Density Functional Theory. *J. Chem. Phys.* **2012**, *136*, 024107.
(42) Bernard, Y. A.; Shao, Y.; Krylov, A. I. General Formulation of Spin-Flip Time-Dependent Density Functional Theory Using Non-Collinear Kernels: Theory, Implementation, and Benchmarks. *J. Chem. Phys.* **2012**, *136*, 204103.
(43) Li, Z.; Liu, W. Spin-Adapted Open-Shell Random Phase Approximation and Time-Dependent Density Functional Theory. I. Theory. *J. Chem. Phys.* **2010**, *133*, 064106.
(44) Li, Z.; Liu, W.; Zhang, Y.; Suo, B. Spin-Adapted Open-Shell Time-Dependent Density Functional Theory. II. Theory and Pilot Application. *J. Chem. Phys.* **2011**, *134*, 134101.
(45) Li, Z.; Liu, W. Spin-Adapted Open-Shell Time-Dependent Density Functional Theory. III. An Even Better and Simpler Formulation. *J. Chem. Phys.* **2011**, *135*, 194106.
(46) Yang, Y.; van Aggelen, H.; Yang, W. Double, Rydberg and Charge Transfer Excitations from Pairing Matrix Fluctuation and

DOI: 10.1021/jp512727a
J. Phys. Chem. A 2015, 119, 4923−4932

Particle−Particle Random Phase Approximation. *J. Chem. Phys.* **2013**, *139*, 224105.
(47) Peng, D.; van Aggelen, H.; Yang, Y.; Yang, W. Linear-Response Time-Dependent Density-Functional Theory with Pairing Fields. *J. Chem. Phys.* **2014**, *140*, 18A522.
(48) Yang, Y.; Peng, D.; Lu, J.; Yang, W. Excitation Energies from Particle−Particle Random Phase Approximation: Davidson Algorithm and Benchmark Studies. *J. Chem. Phys.* **2014**, *141*, 124104.
(49) Zhang, D.; Peng, D.; Zhang, P.; Yang, W. Analytic Gradients, Geometry Optimization and Excited State Potential Energy Surfaces from the Particle−Particle Random Phase Approximation. *Phys. Chem. Chem. Phys.* **2015**, *17*, 1025−1038.
(50) Peng, D.; Yang, Y.; Zhang, P.; Yang, W. Restricted Second Random Phase Approximations and Tamm−Dancoff Approximations for Electronic Excitation Energy Calculations. *J. Chem. Phys.* **2014**, *141*, 214102.
(51) Ring, P.; Schuck, P. *The Nuclear Many-Body Problem*; Physics and Astronomy Online Library; Springer: New York, 2004.
(52) Rowe, D. J. Equations-of-Motion Method and the Extended Shell Model. *Rev. Mod. Phys.* **1968**, *40*, 153−166.
(53) van Aggelen, H.; Yang, Y.; Yang, W. Exchange-Correlation Energy from Pairing Matrix Fluctuation and the Particle−Particle Random-Phase Approximation. *Phys. Rev. A* **2013**, *88*, 030501.
(54) van Aggelen, H.; Yang, Y.; Yang, W. Exchange-Correlation Energy from Pairing Matrix Fluctuation and the Particle−Particle Random Phase Approximation. *J. Chem. Phys.* **2014**, *140*, 18A511.
(55) Sattelmeyer, K. W., III; H.F, S.; Stanton, J. F. Use of 2h and 3h-p-like Coupled-Cluster Tamm−Dancoff Approaches for the Equilibrium Properties of Ozone. *Chem. Phys. Lett.* **2003**, *378*, 42−46.
(56) Shen, J.; Piecuch, P. Doubly Electron-Attached and Doubly Ionized Equation-of-Motion Coupled-Cluster Methods with 4-Particle−2-Hole and 4-Hole−2-Particle Excitations and Their Active-Space Extensions. *J. Chem. Phys.* **2013**, *138*, 194102.
(57) Lee, C.; Yang, W.; Parr, R. G. Development of the Colle−Salvetti Correlation-Energy Formula into a Functional of the Electron Density. *Phys. Rev. B* **1988**, *37*, 785−789.
(58) Becke, A. D. Density-Functional Thermochemistry. III. The Role of Exact Exchange. *J. Chem. Phys.* **1993**, *98*, 5648−5652.
(59) Perdew, J. P.; Burke, K.; Ernzerhof, M. Generalized Gradient Approximation Made Simple. *Phys. Rev. Lett.* **1996**, *77*, 3865−3868.
(60) Yang, Y.; van Aggelen, H.; Steinmann, S. N.; Peng, D.; Yang, W. Benchmark Tests and Spin Adaptation for the Particle−Particle Random Phase Approximation. *J. Chem. Phys.* **2013**, *139*, 174110.
(61) An in-house program for QM/MM simulations
(62) See Supporting Information.
(63) Herzberg, G., Huber, K. *Molecular Spectra and Molecular Structure: Constants of Diatomic Molecules*; Molecular Spectra and Molecular Structure; Van Nostrand Reinhold: New York, 1979.
(64) Mulliken, R. S. Electronic Structures of Polyatomic Molecules and Valence. II. Quantum Theory of the Double Bond. *Phys. Rev.* **1932**, *41*, 751−758.
(65) Herzberg, G.; Shoosmith, J. Spectrum and Structure of the Free Methylene Radical. *Nature* **1959**, *183*, 1801−1802.
(66) Harrison, J. F. Structure of Methylene. *Acc. Chem. Res.* **1974**, *7*, 378−384.
(67) Shavitt, I. Geometry and Singlet-Triplet Energy Gap in Methylene: A Critical Review of Experimental and Theoretical Determinations. *Tetrahedron* **1985**, *41*, 1531−1542.
(68) Shih, S.-K.; Peyerimhoff, S. D.; Buenker, R. J.; Perić, M. Calculation of the Electron Affinity and 1A1-3B1T0 Value of Methylene Using the ab Initio MRD CI Method for a Large AO Basis. *Chem. Phys. Lett.* **1978**, *55*, 206−212.
(69) Jarzecki, A. A.; Davidson, E. R. Does Unrestricted Møller−Plesset Perturbation Theory for Low Spin Converge When the System Has a Triplet Ground State? *J. Phys. Chem. A* **1998**, *102*, 4742−4746.
(70) Gu, J.-P.; Hirsch, G.; Buenker, R.; Brumm, M.; Osmann, G.; Bunker, P.; Jensen, P. A Theoretical Study of the Absorption Spectrum of Singlet CH_2. *J. Mol. Struct.* **2000**, *517 - 518*, 247−264.
(71) Osmann, G.; Bunker, P.; Jensen, P.; Kraemer, W. An ab Initio Study of the NH_2+ Absorption Spectrum. *J. Mol. Spectrosc.* **1997**, *186*, 319−334.
(72) Berkowitz, J.; Greene, J. P.; Cho, H.; Ruščić, B. Photoionization Mass Spectrometric Studies of SiH_n (n = 1−4). *J. Chem. Phys.* **1987**, *86*, 1235−1248.
(73) Escribano, R.; Campargue, A. Absorption Spectroscopy of SiH_2 near 640 nm. *J. Chem. Phys.* **1998**, *108*, 6249−6257.
(74) Berkowitz, J.; Cho, H. A Photoionization Study of PH:PH2 Revisited. *J. Chem. Phys.* **1989**, *90*, 1−6.
(75) Borden, W. T.; Davidson, E. R. Theoretical Studies of Diradicals Containing Four π Electrons. *Acc. Chem. Res.* **1981**, *14*, 69−76.
(76) Dowd, P. Trimethylenemethane. *J. Am. Chem. Soc.* **1966**, *88*, 2587−2589.
(77) Feller, D.; Tanaka, K.; Davidson, E. R.; Borden, W. T. Potential Surface for the Methylenecyclopropane Rearrangement. *J. Am. Chem. Soc.* **1982**, *104*, 967−972.
(78) Feller, D.; Davidson, E. R.; Borden, W. T. Ab Initio CI Calculations of the Energy Difference between Trimethylenemethane and Butadiene. *Isr. J. Chem.* **1983**, *23*, 105−108.
(79) Ma, B., III; H.F, S. Singlet−Triplet Energy Separation and Barrier for Ring Closure for Trimethylenemethane and Its Complexes. *Chem. Phys.* **1996**, *207*, 31−41.
(80) Wenthold, P. G.; Hu, J.; Squires, R. R.; Lineberger, W. C. Photoelectron Spectroscopy of the Trimethylene−Methane Negative Ion. The Singlet-Triplet Splitting of Trimethylenemethane. *J. Am. Chem. Soc.* **1996**, *118*, 475−476.
(81) Cramer, C. J.; Smith, B. A. Trimethylenemethane. Comparison of Multiconfiguration Self-Consistent Field and Density Functional Methods for a Non-Kekulé Hydrocarbon. *J. Phys. Chem.* **1996**, *100*, 9664−9670.
(82) Slipchenko, L. V.; Krylov, A. I. Electronic Structure of the Trimethylenemethane Diradical in Its Ground and Electronically Excited States: Bonding, Equilibrium Geometries, and Vibrational Frequencies. *J. Chem. Phys.* **2003**, *118*, 6874−6883.
(83) Allinger, N.; Gilardeau, C.; Chow, L. Organic Quantum Chemistry XVI: A Theoretical Study of the Structures and Electronic Spectra of Cyclobutadiene and Dimethylenecyclobutene. *Tetrahedron* **1968**, *24*, 2401−2406.
(84) Buenker, R. J.; Peyerimhoff, S. D. Ab Initio Study on the Stability and Geometry of Cyclobutadiene. *J. Chem. Phys.* **1968**, *48*, 354−373.
(85) Borden, W. T.; Davidson, E. R.; Hart, P. The Potential Surfaces for the Lowest Singlet and Triplet States of Cyclobutadiene. *J. Am. Chem. Soc.* **1978**, *100*, 388−392.
(86) Bally, T.; Masamune, S. Cyclobutadiene. *Tetrahedron* **1980**, *36*, 343−370.
(87) Filatov, M.; Shaik, S. Application of Spin-Restricted Open-Shell Kohn−Sham Method to Atomic and Molecular Multiplet States. *J. Chem. Phys.* **1999**, *110*, 116−125.
(88) Lyakh, D. I.; Lotrich, V. F.; Bartlett, R. J. The 'Tailored' CCSD(T) Description of the Automerization of Cyclobutadiene. *Chem. Phys. Lett.* **2011**, *501*, 166−171.
(89) Boguslawski, K.; Tecmer, P.; Bultinck, P.; De Baerdemacker, S.; Van Neck, D.; Ayers, P. W. Nonvariational Orbital Optimization Techniques for the AP1roG Wave Function. *J. Chem. Theory Comput.* **2014**, *10*, 4873−4882.
(90) Eckert-Maksić, M.; Vazdar, M.; Barbatti, M.; Lischka, H.; Maksić, Z. B. Automerization Reaction of Cyclobutadiene and Its Barrier Height: an ab Initio Benchmark Multireference Average-Quadratic Coupled Cluster Study. *J. Chem. Phys.* **2006**, *125*, 064310.
(91) Clark, A. E.; Davidson, E. R. Model Studies of Hydrogen Atom Addition and Abstraction Processes Involving ortho-, meta-, and para-Benzynes. *J. Am. Chem. Soc.* **2001**, *123*, 10691−10698.
(92) Clark, A. E.; Davidson, E. R. Local Spin III: Wave Function Analysis along a Reaction Coordinate, H Atom Abstraction, and Addition Processes of Benzyne. *J. Phys. Chem. A* **2002**, *106*, 6890−6896.

DOI: 10.1021/jp512727a
J. Phys. Chem. A 2015, 119, 4923−4932

(93) Clark, A. E.; Davidson, E. R. p-Benzyne Derivatives That Have Exceptionally Small Singlet-Triplet Gaps and Even a Triplet Ground State. *J. Org. Chem.* **2003**, *68*, 3387−3396.
(94) Wenthold, P. G.; Squires, R. R.; Lineberger, W. C. Ultraviolet Photoelectron Spectroscopy of the *o*-, *m*-, and *p*-Benzyne Negative Ions. Electron Affinities and Singlet-Triplet Splittings for *o*-, *m*-, and *p*-Benzyne. *J. Am. Chem. Soc.* **1998**, *120*, 5279−5290.

DOI: 10.1021/jp512727a
J. Phys. Chem. A 2015, 119, 4923−4932